



Natural radionuclides and radiological risk assessment in the stream and river sediments of a high background natural radiation area Kanyakumari, India

Thennaarassan Natarajan · Sarata Kumar Sahoo · Kazumasa Inoue · Hideki Arae · Tatsuo Aono · Masahiro Fukushi

Received: 26 November 2023 / Accepted: 12 February 2024 / Published online: 1 March 2024
© The Author(s), under exclusive licence to Springer Nature Switzerland AG 2024

Abstract The Kanyakumari coast is known to be a high background natural radiation area due to the placer deposits of heavy minerals such as ilmenite, monazite, and rutile. The Kanyakumari river sediments that could be the source of the elevated amounts of natural radionuclides in the coastal sands have been studied in this paper. The activity concentrations of primordial radionuclides ^{226}Ra , ^{232}Th , and ^{40}K were determined using high-purity germanium (HPGe) gamma-ray spectrometry. The mean activity concentrations of ^{226}Ra , ^{232}Th , and ^{40}K were found to be 75 Bq kg^{-1} , 565 Bq kg^{-1} , and 360 Bq kg^{-1} , respectively. The mean absorbed dose rate was 395 nGy h^{-1} . Radiological hazard parameters were studied and compared with the world average values. The contribution of ^{232}Th to the total dose rate was found to be higher than that of the two other radionuclides.

The high mean ratio of $^{232}\text{Th}/^{226}\text{Ra}$ suggested an enrichment of ^{232}Th and the occurrence of ^{226}Ra leaching due to an oxidizing environment. Principal component analysis (PCA) was carried out for the radionuclides in order to discriminate the source of the sediments. This study provides new insights into the distribution of natural radionuclides in sediments of rivers and streams.

Keywords Natural radionuclides · River sediments · Thorium · Radiological hazard parameters · Absorbed dose rate · Gamma spectrometry

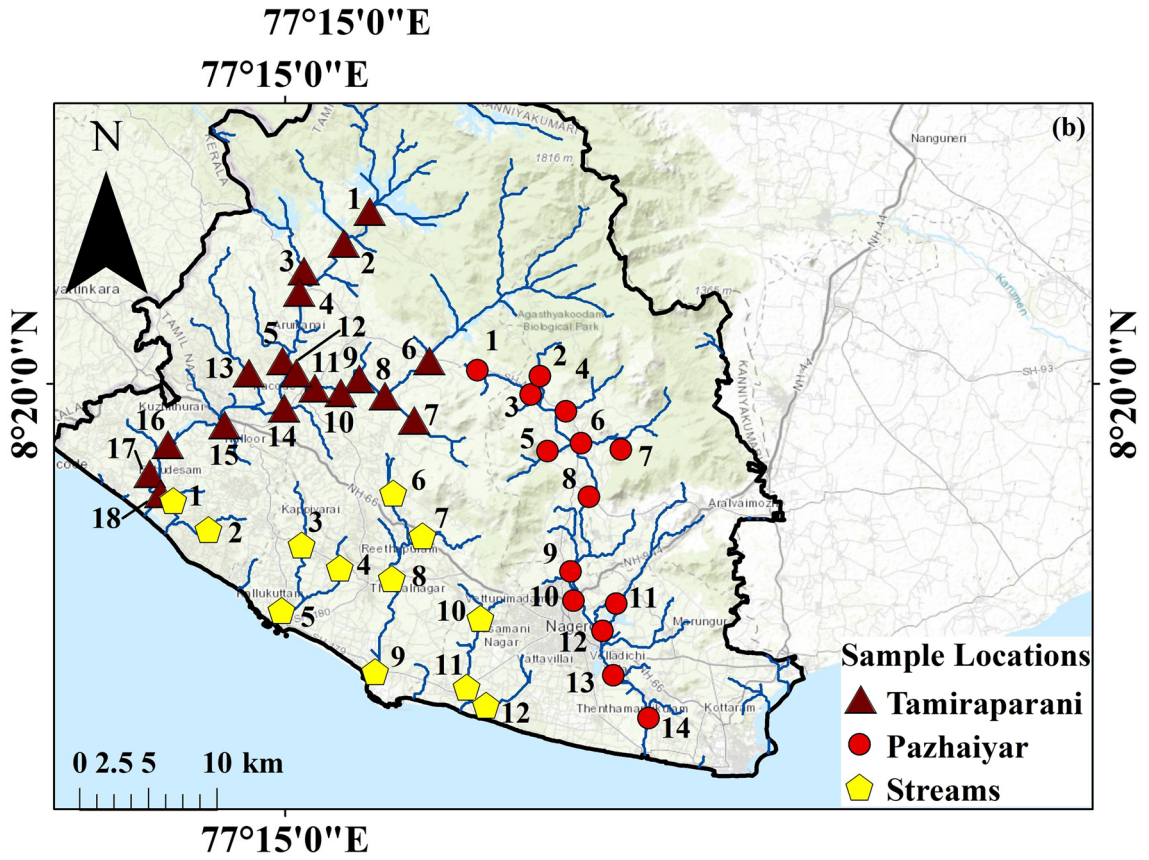
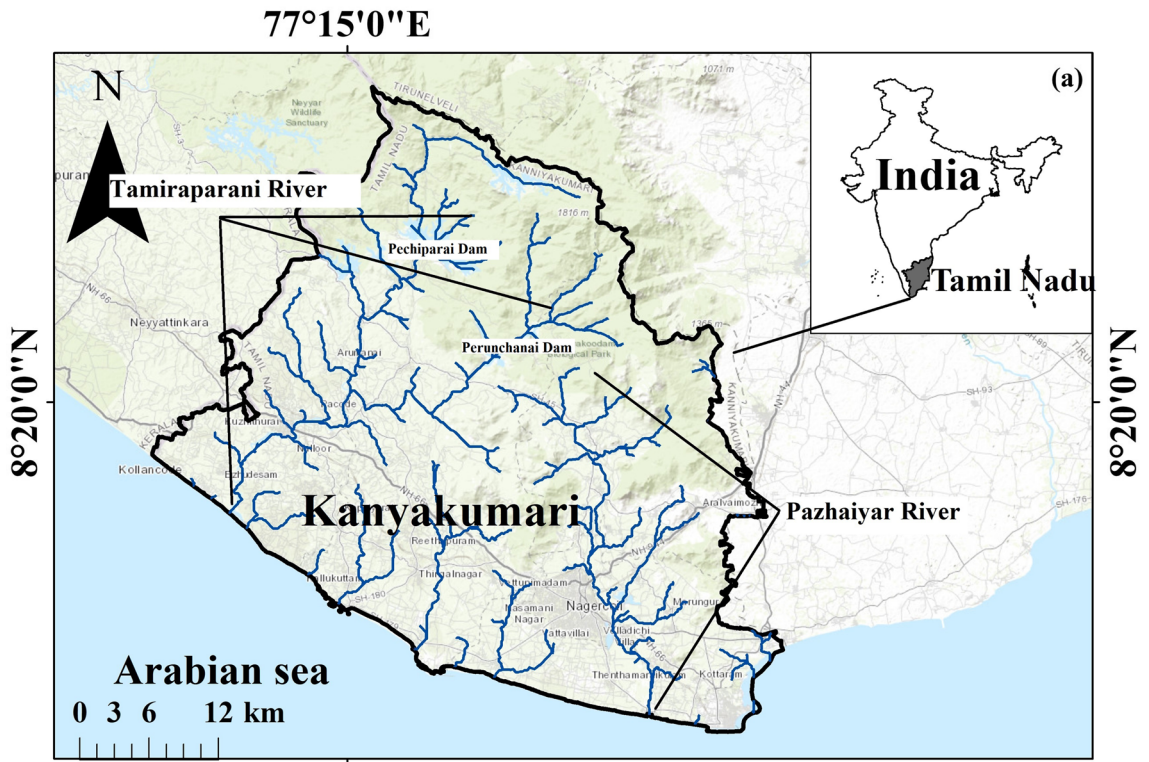
Introduction

Naturally occurring radioactive materials (NORMs) existing in sufficient quantity with their decay products are significant sources of radiation exposure for the human population. These NORMs can be found across the earth's crust causing terrestrial environmental radioactivity. The external exposure to humans is mainly due to the primordial radionuclides of the ^{238}U and ^{232}Th decay series as well as ^{40}K (UNSCEAR (United Nations Scientific Committee on the Effects of Atomic Radiation), 2000). A mitochondrial DNA mutation associated with the exposure to natural radioactivity has been reported for the human inhabitants along the Chavara-Neendakara coast of Kerala, India (Forster et al., 2002). Such type of data escalates the importance to understand the

T. Natarajan · K. Inoue · M. Fukushi
Department of Radiological Sciences, Graduate School of Human Health Sciences, Tokyo Metropolitan University, Arakawa-Ku, Tokyo 116-8551, Japan

T. Natarajan · S. K. Sahoo (✉) · H. Arae · T. Aono
Institute for Radiological Sciences, National Institutes for Quantum Science and Technology (QST), Inage-Ku, Chiba 263-8555, Japan
e-mail: sahoosarata@qst.go.jp

T. Aono
Radioecology Unit, Fukushima Institute for Research, Education and Innovation (F-REI), Fukushima 960-1295, Japan



◀**Fig. 1** Kanyakumari district maps **a** showing rivers and streams and **b** showing sediment sampling locations ($n=44$) (Generated using ArcGIS 10.6 software) (Numeric value in the river Sample ID are assigned from low to high for the catchment area to the mouth of the river)

distribution of NORMs in the environment in association with radiological hazards and human health risks.

Regions with enormous amounts of the primordial radionuclides associated with rocks, soil, and sand are identified as high background natural radiation areas (HBNRAs). There are a few well-known HBNRAs; however, the sources of natural radionuclides vary according to the local geology and geological processes. For example, in Ramsar, Iran, and Niška Banja, Serbia, these radionuclides are associated with travertine formations; in the Abu Rusheid area of Egypt, they are linked to mylonitic rocks with U mineralization; and in the Dornogobi Province of south-eastern Mongolia, the presence of U deposits close to the ground surface has resulted in high dose rates (Ghiassi-nejad et al., 2002; Omori et al., 2019; Sahoo et al., 2023; Sakr et al., 2023). In coastal regions of India, high background natural radiation is associated with beach placer deposits of heavy minerals (density (ρ) $> 2.9 \text{ g cm}^{-3}$) such as ilmenite, monazite, rutile, and zircon (Mohanty et al., 2003; Veerasamy et al., 2020). Especially the thorium-bearing mineral monazite is considered to be the highest contributor to the background radiation in the beach sands of India (Mohanty et al., 2003; Singh et al., 2007; Veerasamy et al., 2020).

The streams and rivers of these coastal areas play a major role in the formation of beach placer deposits. The hinterland high-grade metamorphic and igneous rocks are weathered and eroded by the streams and rivers, and the detritus composed of sand, silt, clay, and heavy minerals is carried and deposited in a variety of coastal environments including deltas, barrier islands, lagoons, foreshore, and backshore. The sediments are then reworked by waves, tides, longshore currents, and winds leading to an effective sorting of the mineral grains based on their size and density (Van Gosen et al., 2014). For instance, the Rushikulya River in Odisha erodes the Eastern Ghat Mobile Belt (EGMB) composed of rock types such as khondalite, charnockite, granite gneiss, and pegmatites and the river is believed to be the source of

heavy minerals and high background natural radioactivity along Chhatrapur beach (Sulekha Rao & Misra, 2009; Veerasamy et al., 2020). Similarly, sediments of the Bentota River in Sri Lanka have been found to be rich in monazite and that has resulted in forming seasonal monazite-rich beach sand deposits along the Kaikawala and Beruwala coastal regions (Rupasinghe et al., 1983).

River sediments (mainly as sand) also have an essential role in construction projects as an important mixture component for building materials in Tamil Nadu, India (Ramasamy et al., 2011). The activity concentration of radionuclides and radiological hazard parameters have been estimated and found to be equal to or less than the world average values in some sediments of the major rivers of Tamil Nadu (Narayana et al., 2016; Ramasamy et al., 2011; Thangam et al., 2020). Natural radionuclide distribution in the coastal sands and soils of the Kanyakumari HBNRA region has been extensively studied (Malathi et al., 2005; Natarajan et al., 2023a; Punniyakotti & Ponnusamy, 2018). However, there is little information about natural radionuclide data in river sediments from this area.

Rivers are a possible source for the high radioactivity observed along the Kanyakumari coastal area. Therefore, in this study, the sediments from rivers and streams of Kanyakumari were analyzed for the activity concentration of natural radionuclides and the radiological hazard parameters were estimated based on data of the natural radionuclides. In addition to it, spatial distribution maps of the natural radionuclides and dose rate were generated to visualize the distribution pattern.

Materials and methods

Study area

Kanyakumari is located at the southernmost tip of India and has two perennial rivers, the Tamiraparani (TR) and the Pazhaiyar (PR). The TR originates as the Kothaiyar River on the Agastiar Hills of Western Ghats and flows on the western slopes for a short distance before taking a southwesterly direction. The Paraliyar River originating from the same hills flows in a southwesterly direction and unites with the Kothaiyar River near Moovattumugam to flow as

the TR until it joins the Arabian Sea near Thengapattinam without forming any delta (Fig. 1a). The PR originating from the Mahendragiri Hills flows on the easterly slopes before taking a southeasterly direction for 30 km to enter the Arabian Sea near Manakudi by forming an estuary. The Kothaiyar, Paraliyar, and TR collectively flow for a length of 60 km from the foothills of the catchment area to reach the mouth (the place where the river enters the sea) and they are grouped as the TR in this study (Fig. 1b).

Kanyakumari receives rainfall from both southwest and northeast monsoons which benefits the rivers; however, most of its precipitation is due to the cyclonic activities in the Bay of Bengal (CGWB, CGWB (Central Groundwater Board of India), 2008). The geology of Kanyakumari is comprised of Trivandrum Block (TB) and Nagercoil granulites (NG) of the Southern Granulite Terrain and the composition of these rocks is discussed in detail elsewhere (Rajesh et al., 2011; Santosh et al., 2003). The catchment area of the rivers includes Precambrian crystalline rocks of charnockites, khondalites, and migmatite gneisses. The rivers erode these rocks which are tonalite-granodiorite in composition with apatite, ilmenite, monazite, and zircon as major accessory minerals (Rajesh et al., 2011). Along with these two major rivers, there are a few small seasonal streams (SS) with a length not exceeding 20 km which form and enter the Arabian Sea. All these streams might once have been the channels of rivers like the TR and Paraliyar as there is evidence for river migration such as oxbow lake (Fig. 2). The width of these stream channels exceeds 100 m in some places and these channels are primarily used for agricultural activities since most of Kanyakumari is rough terrain, unsuited to farming (Fig. 3a, b). Figure 3c shows the cross section at a SS sampling location indicating the river depositional sequence.

Sample preparation

Sediment samples were collected from the foothills of the catchment area to the mouth of the rivers at 18 locations for the TR and at 14 for the PR. Sediment samples were also collected at 12 locations for the SS among the agricultural lands (Table 1). All the sampling locations were within latitude N 8.114 to 8.446 and longitude E 77.161 to 77.488 and sampling was done during March 2022 (summer season). For

the TR and PR, the interval between each sampling location along the main channel was approximately maintained at 2 km. Since both rivers have tributaries joining them, sediment samples from those tributaries were also collected, respectively (Fig. 1b). The SS sediment samples were collected from the branches before and after confluence (Fig. 1b). The samples from each location were collected at a depth of 0–5 cm using a Wildco® hand core sediment sampler and stored in a labelled polyethylene bag before being transported to the laboratory in Japan. The sediment samples were brought to Japan after acquiring proper permission from the Ministry of Agriculture, Forestry and Fisheries based on plant protection laws. In the laboratory, each sediment sample was first air-dried and then oven-dried at 105 °C for 24 h until complete removal of moisture had been realized. Plant root materials and rock fragments were removed by passing the dried samples through a 2-mm sieve. The samples were packed and sealed in U8 cylindrical containers ($d=48$ mm, $h=58$ mm) and left for 4 weeks to attain secular equilibrium among the U series radionuclides.

Instrumentation and calibration

A coaxial P-type high-purity germanium (HPGe) detector (CANBERRA GX4018) with a range of 0–4000 keV was used for gamma spectrometry measurements. Energy and efficiency calibration of the HPGe detector was carried out using a multi-nuclide standard source supplied by the Japan Radioisotope Association (JRIA) with gamma energies ranging from 60 to 1333 keV and the overall uncertainty was found to be less than 10%. The precision of the method was checked using the reference material Irish Sea Sediment IAEA – 385. The sample counting time was pre-set at 80,000 s. ^{214}Pb (351.99 keV) and ^{214}Bi (609.31 keV) were considered for the estimation of ^{226}Ra activity concentration. ^{208}Tl (583.14 keV) and ^{228}Ac (911.20 keV) peaks were considered for the calculation of ^{232}Th , assuming that the daughter radionuclides are in radioactive equilibrium with parent radionuclides and ^{40}K (1460.8 keV) was considered for the direct estimation of ^{40}K activity concentration (Natarajan et al., 2023a). The minimum detection levels (MDL) for ^{214}Pb and ^{214}Bi were 2 ± 1 Bq kg^{-1} and 2 ± 1 Bq kg^{-1} , ^{208}Tl and ^{228}Ac

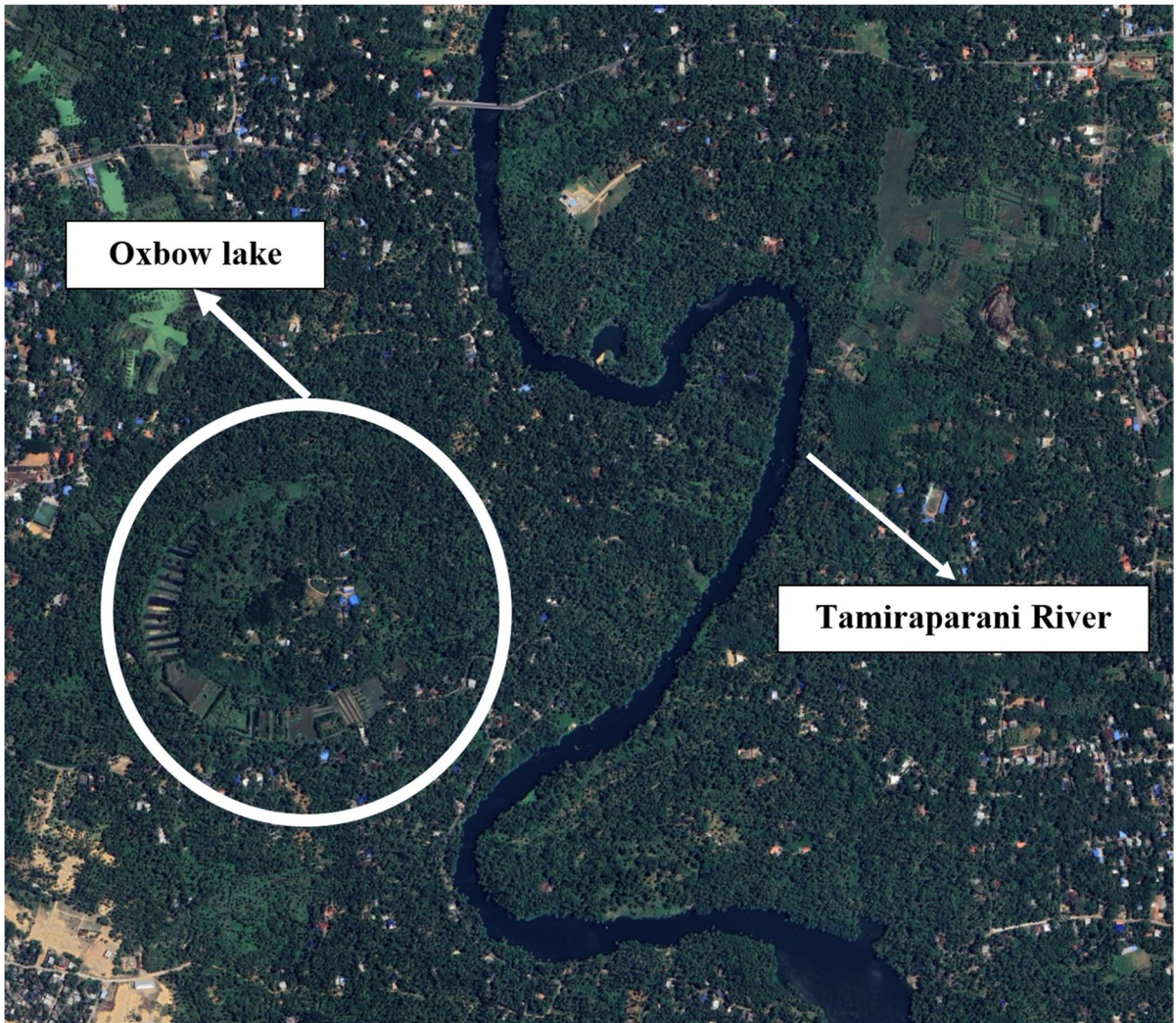


Fig. 2 Satellite image of an oxbow lake adjacent to the Tamiraparani River demonstrating migration of the river (Google Earth Version 9.191.0.0)

were $3 \pm 2 \text{ Bq kg}^{-1}$ and $3 \pm 1 \text{ Bq kg}^{-1}$, and the MDL for ^{40}K was $11 \pm 5 \text{ Bq kg}^{-1}$, respectively. The specific activities (Bq kg^{-1}) were calculated using Eq. (1).

$$A = \frac{C}{pw t \epsilon} \tag{1}$$

Here, A is the specific activity, C is the net count above the background, p is the absolute emission probability, w is the dry weight of sample (kg), t is the measurement time (80,000 s), and ϵ is the absolute efficiency of the detector (Hassan et al., 2010).

Spatial analysis

The spatial distribution maps were prepared using ArcGIS software (v 10.6). The inverse distance weighted (IDW) method in the software Spatial Analyst Tool was used to determine the values for unsampled locations. The IDW method presumes that every measured point has an effect that decreases with distance and the nearest value is considered rather than the farthest away one. Although inverse distance weighting (IDW), ordinary kriging (OK), and ordinary co-kriging (OCK)

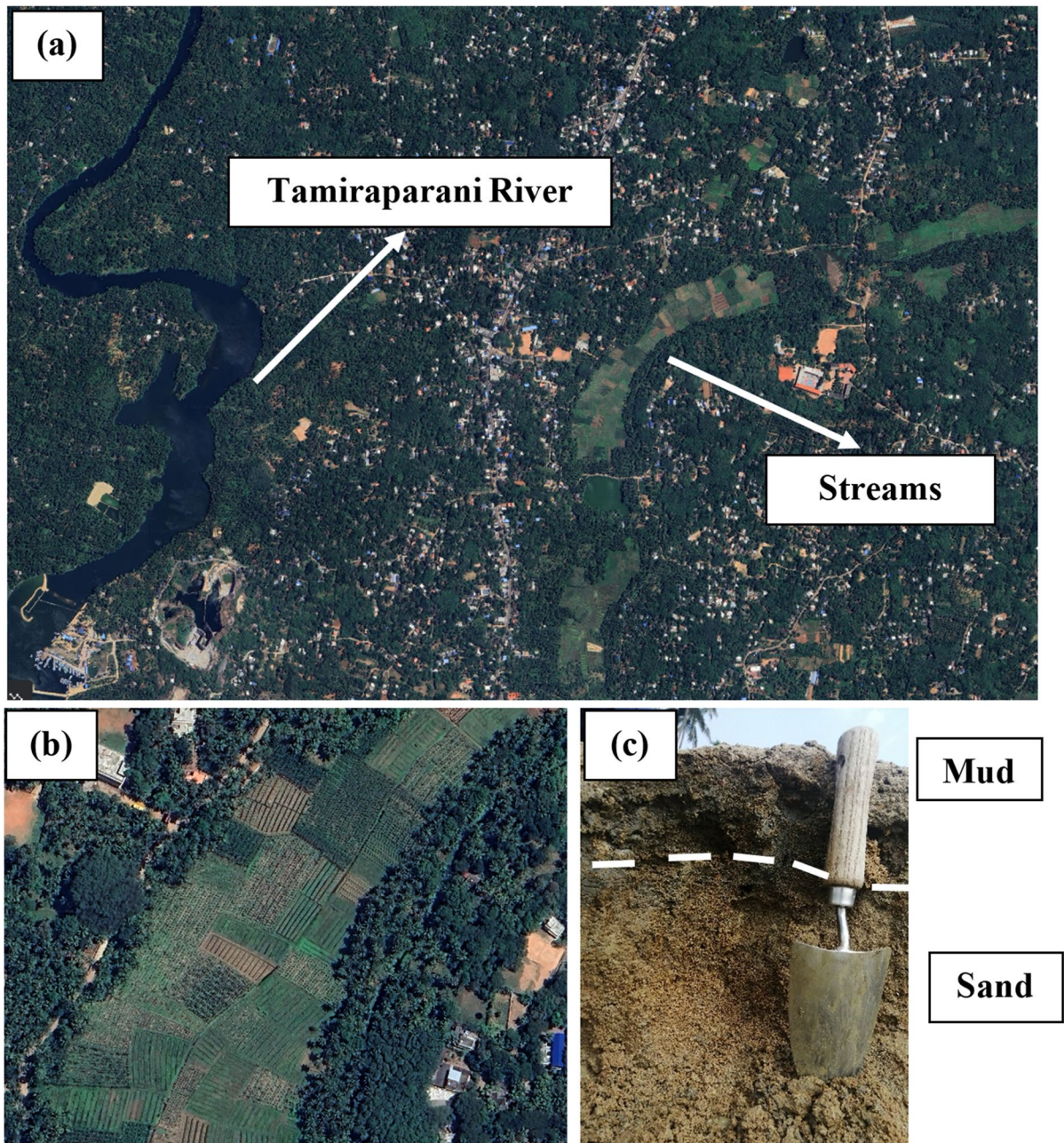


Fig. 3 Satellite images of **a** streams and **b** agricultural activities on the old river channels (Google Earth Version 9.191.0.0). **c** Cross section at a stream sampling location showing the river depositional sequence

methods are more commonly used, for this study, the IDW method was employed since it has been found to be the best conventional interpolation technique with some measure of certainty and

predictive accuracy (Li & Heap, 2011). The boundary for the spatial distribution starts from the foothills, from where the first sampling location was found.

Table 1 Activity concentration (Bq kg⁻¹) of ²²⁶Ra, ²³²Th, and ⁴⁰K with absorbed dose rate (nGy h⁻¹) for Kanyakumari River and stream sediment samples

Sample ID	Latitude (N)	Longitude (E)	Activity concentration (Bq kg ⁻¹)			Absorbed dose rate (nGy h ⁻¹)
			²²⁶ Ra	²³² Th	⁴⁰ K	
Tamiraparani River sediments (n = 18)						
TR-1	8.446	77.305	28	207	444	157
TR-2	8.425	77.288	29	223	166	155
TR-3	8.407	77.262	386	1580	127	1138
TR-4	8.393	77.259	185	1985	96	1288
TR-5	8.348	77.248	51	147	587	137
TR-6	8.348	77.344	192	2362	65	1518
TR-7	8.309	77.334	19	39	450	51
TR-8	8.325	77.315	22	107	632	101
TR-9	8.342	77.298	162	1837	93	1188
TR-10	8.327	77.286	57	518	260	350
TR-11	8.330	77.269	81	818	291	544
TR-12	8.340	77.257	211	1860	293	1233
TR-13	8.340	77.226	18	55	194	50
TR-14	8.317	77.249	18	105	530	94
TR-15	8.306	77.210	41	354	329	246
TR-16	8.293	77.173	93	511	586	376
TR-17	8.274	77.161	129	819	346	569
TR-18	8.261	77.168	79	379	613	291
Pazhaiyar River sediments (n = 14)						
PR-1	8.342	77.376	5	12	459	28
PR-2	8.326	77.411	42	136	645	129
PR-3	8.338	77.417	5	19	597	38
PR-4	8.315	77.434	63	617	580	426
PR-5	8.294	77.444	64	490	678	353
PR-6	8.289	77.422	4	40	353	41
PR-7	8.289	77.470	29	459	276	302
PR-8	8.259	77.449	23	174	671	144
PR-9	8.210	77.437	30	209	711	170
PR-10	8.191	77.439	22	128	718	117
PR-11	8.171	77.458	20	143	701	125
PR-12	8.189	77.467	22	221	209	152
PR-13	8.142	77.465	91	1372	215	880
PR-14	8.114	77.488	44	359	359	252
Stream sediments (n = 12)						
SS-1	8.257	77.177	112	572	100	401
SS-2	8.238	77.200	368	2163	48	1478
SS-3	8.228	77.261	19	95	219	75
SS-4	8.213	77.286	53	267	216	194
SS-5	8.185	77.248	110	516	108	367
SS-6	8.262	77.321	146	677	146	482
SS-7	8.234	77.340	26	147	659	128
SS-8	8.206	77.320	132	1197	370	799
SS-9	8.145	77.309	105	709	258	487
SS-10	8.180	77.378	26	139	272	108

Table 1 (continued)

Sample ID	Latitude (N)	Longitude (E)	Activity concentration (Bq kg ⁻¹)			Absorbed dose rate (nGy h ⁻¹)
			²²⁶ Ra	²³² Th	⁴⁰ K	
SS-11	8.135	77.369	12	69	111	52
SS-12	8.123	77.382	26	132	28	93

Radiological hazard parameters

The radiological hazard parameters such as absorbed dose rate (D), annual effective dose equivalent ($AEDE$), and radium equivalent (Ra_{eq}) were estimated based on the activity concentrations of ²²⁶Ra, ²³²Th, and ⁴⁰K in order to assess the radiological risk of the river and stream sediments. The radiological effects are directly related to D (nGy h⁻¹) and D was calculated using Eq. (2) suggested by the UNSCEAR (UNSCEAR (United Nations Scientific Committee on the Effects of Atomic Radiation), 2000).

$$D = 0.462C_{Ra} + 0.604C_{Th} + 0.0417C_K \quad (2)$$

Here, C_{Ra} , C_{Th} , and C_K are the activity concentrations of ²²⁶Ra, ²³²Th, and ⁴⁰K, respectively.

The river sediments are mainly used as materials to be mixed with cement for building construction. As people spend more time indoors than outdoors, the annual dose to any individual can be assessed by calculating the annual effective dose equivalent ($AEDE$) outdoors and indoors by Eqs. (3) and (4) as given by the UNSCEAR (United Nations Scientific Committee on the Effects of Atomic Radiation) (2000).

$$AEDE_{out} = D \times 8760 \times 0.2 \times 0.7 \times 10^{-6} \quad (3)$$

$$AEDE_{in} = D \times 8760 \times 0.8 \times 0.7 \times 10^{-6} \quad (4)$$

Here, $AEDE_{out}$ and $AEDE_{in}$ (mSv y⁻¹) are for the outdoor and indoor effective dose equivalents, respectively; D is the absorbed dose rate; 0.7 Sv Gy⁻¹ is used to convert the absorbed dose rate (nGy h⁻¹) to the annual effective dose equivalent. Finally, 0.2 and 0.8 are the occupancy factors of outdoors and indoors.

Radium equivalent activity (Ra_{eq}) is a widely used hazard index. This single index allows assessment of the exposure to radiation since the radionuclides ²²⁶Ra, ²³²Th, and ⁴⁰K are not uniformly distributed in the river and stream sediments. Ra_{eq} can be calculated

using Eq. (5) (UNSCEAR (United Nations Scientific Committee on the Effects of Atomic Radiation), 2000) and it is expressed in Bq kg⁻¹.

$$Ra_{eq} = C_{Ra} + 1.43C_{Th} + 0.077C_K \quad (5)$$

Here, C_{Ra} , C_{Th} , and C_K are the activity concentrations of ²²⁶Ra, ²³²Th, and ⁴⁰K, respectively.

Results and discussion

Activity concentration

Activity concentrations of ²²⁶Ra, ²³²Th, and ⁴⁰K (Bq kg⁻¹) of the river and stream sediments are given in Table 1. The activity concentrations of ²²⁶Ra, ²³²Th, and ⁴⁰K (Bq kg⁻¹) for the TR sediment samples ($n=18$) were in the range of 18 to 386 with a mean of 100 Bq kg⁻¹, 39 to 2362 with a mean of 773 Bq kg⁻¹, and 65 to 632 with a mean of 340 Bq kg⁻¹, respectively. The activity concentrations of ²²⁶Ra, ²³²Th, and ⁴⁰K (Bq kg⁻¹) for the PR sediment samples ($n=14$) ranged from 4 to 91 with a mean of 33 Bq kg⁻¹, 12 to 1372 with a mean of 313 Bq kg⁻¹, and 209 to 718 with a mean of 512 Bq kg⁻¹. The activity concentrations of ²²⁶Ra, ²³²Th, and ⁴⁰K (Bq kg⁻¹) for the SS sediments ($n=12$) ranged from 12 to 368 with a mean of 95 Bq kg⁻¹, 69 to 2163 with a mean of 557 Bq kg⁻¹, and 28 to 659 with a mean of 211 Bq kg⁻¹. The mean activity concentrations of ²³²Th (Bq kg⁻¹) of both rivers and stream sediments were found to be relatively higher than the world average value of 45 Bq kg⁻¹ as well as the Indian average value of 68 Bq kg⁻¹ (UNSCEAR, 2008; Punniyakotti & Ponnusamy, 2018). In case of ²²⁶Ra activity concentration, the TR and SS sediments were found to be higher than the world average value of 33 Bq kg⁻¹ and Indian average value of 28 Bq kg⁻¹, whereas the mean ²²⁶Ra activity concentration of PR sediments was normal. However, the

mean ^{40}K activity concentration was a little higher than the world average value of 412 Bq kg^{-1} only for the PR sediments.

The mean activity concentration of radionuclides followed the order of $^{232}\text{Th} > ^{40}\text{K} > ^{226}\text{Ra}$ in both TR and SS sediments, whereas it was $^{40}\text{K} > ^{232}\text{Th} > ^{226}\text{Ra}$ for the PR sediments. In the river and stream sediments, ^{226}Ra activity concentration was lower than that of ^{232}Th and ^{40}K ; ^{226}Ra is known to be preferentially incorporated into the aqueous phase by means of alpha recoil, and this could be a possible reason for the depletion of ^{226}Ra relative to ^{232}Th in the river and stream sediments (Powell et al., 2007). The soils of the Odisha HBNRA were suspected to be the cause of the increased U concentration in the groundwater (Veerasamy et al., 2023). The river water may also feed the groundwater by influent flows during high flow times. Water is an essential component for the survival of life and the people of Kanyakumari rely more on the groundwater for freshwater needs (Raja et al., 2021). However, the average uranium concentration in the groundwater of Kanyakumari was found to be $2 \mu\text{g L}^{-1}$ which was less than the permissible limit recommended by the WHO ($30 \mu\text{g L}^{-1}$) and the Atomic Energy Regulatory Board (AERB) of India ($60 \mu\text{g L}^{-1}$) (Raja et al., 2021).

The high activity concentration of ^{40}K may be owing to the presence of light silicate and felsic groups of minerals as ^{40}K mainly has a terrestrial origin (Natarajan et al., 2023a). The high concentrations of ^{40}K and ^{232}Th compared to ^{226}Ra have also been observed in other river sediments of Tamil Nadu such as the Cauvery, Ponnaiyar, and Thambarani (Tirunelveli) Rivers (Narayana et al., 2016; Ramasamy et al., 2011; Thangam et al., 2020). A similar observation was reported in the Nile River (Egypt) sediments and it was stated that the clay content might be a contributing factor for the high activity concentrations of ^{40}K , while conversely the lower concentrations were associated with sandy content (El-Gamal et al., 2007). The major rock types present in the catchment area of the TR and PR might also influence the activity concentrations of ^{226}Ra , ^{232}Th , and ^{40}K since they are rich in heavy minerals like ilmenite, monazite, and zircon as the major accessory phase. Natural radiation levels as high as $45,000 \text{ nGy h}^{-1}$ have been reported in hinterland Putteti syenite rock units and the western part of the Kanyakumari

district also exhibited a prominent radioactivity zone (Singh et al., 2007).

The spatial distributions of the radionuclides ^{226}Ra , ^{232}Th , and ^{40}K are shown in Fig. 4a, b, and c, respectively. A heterogenous distribution of radionuclides was seen. The background radiation levels in the Kanyakumari district were mainly associated with the ^{232}Th because of the presence of thorium-bearing minerals. The spatial distribution map of Fig. 4b indicated that the very high concentrations of ^{232}Th were limited to the western part of this district.

The world average ratios for $^{232}\text{Th}/^{226}\text{Ra}$, $^{232}\text{Th}/^{40}\text{K}$, and $^{226}\text{Ra}/^{40}\text{K}$ are 0.86, 0.08, and 0.09, respectively (UNSCEAR (United Nations Scientific Committee on the Effects of Atomic Radiation), 2000). The mean $^{232}\text{Th}/^{226}\text{Ra}$, $^{232}\text{Th}/^{40}\text{K}$, and $^{226}\text{Ra}/^{40}\text{K}$ ratios of TR and PR sediments were 6.98, 5.99, and 0.68 and 8.10, 0.94, and 0.08, respectively, and for SS sediments, the ratios were 5.65, 6.20, and 1.10, respectively. $^{232}\text{Th}/^{226}\text{Ra}$ and $^{232}\text{Th}/^{40}\text{K}$ ratios were considerably higher than the world average values, and that showed the dominance of the Th-rich minerals in the sediments. The mean $^{226}\text{Ra}/^{40}\text{K}$ ratio of the PR sediments was slightly lower than the world average due to the predominance of light minerals over U-rich minerals and the elevated $^{232}\text{Th}/^{226}\text{Ra}$ of TR, PR, and SS sediments could indicate the leaching of ^{226}Ra due to an oxidizing environment (Khan et al., 2022).

Radiological risk assessment

The absorbed dose rate (D) in air at 1 m above the ground was estimated using Eq. (2) and it ranged from 50 to 1518 nGy h^{-1} with a mean of 527 nGy h^{-1} for TR sediment samples, from 28 to 880 nGy h^{-1} with a mean of 226 nGy h^{-1} for PR sediment samples, and from 52 to 1478 nGy h^{-1} with a mean of 390 nGy h^{-1} for SS sediment samples. The mean absorbed dose rates of river and stream sediments were found to be relatively higher than the world average value of 58 nGy h^{-1} reported by the UNSCEAR (2008). The spatial distribution of the absorbed dose rate is shown in Fig. 4d. The comparison of the activity concentrations of natural radionuclides ^{226}Ra , ^{232}Th , and ^{40}K (Bq kg^{-1}) and absorbed dose rate (nGy h^{-1}) for the river and stream sediment samples from Kanyakumari with some of the river sediments from other locations in India (Tamil Nadu, Kerala, and Odisha)

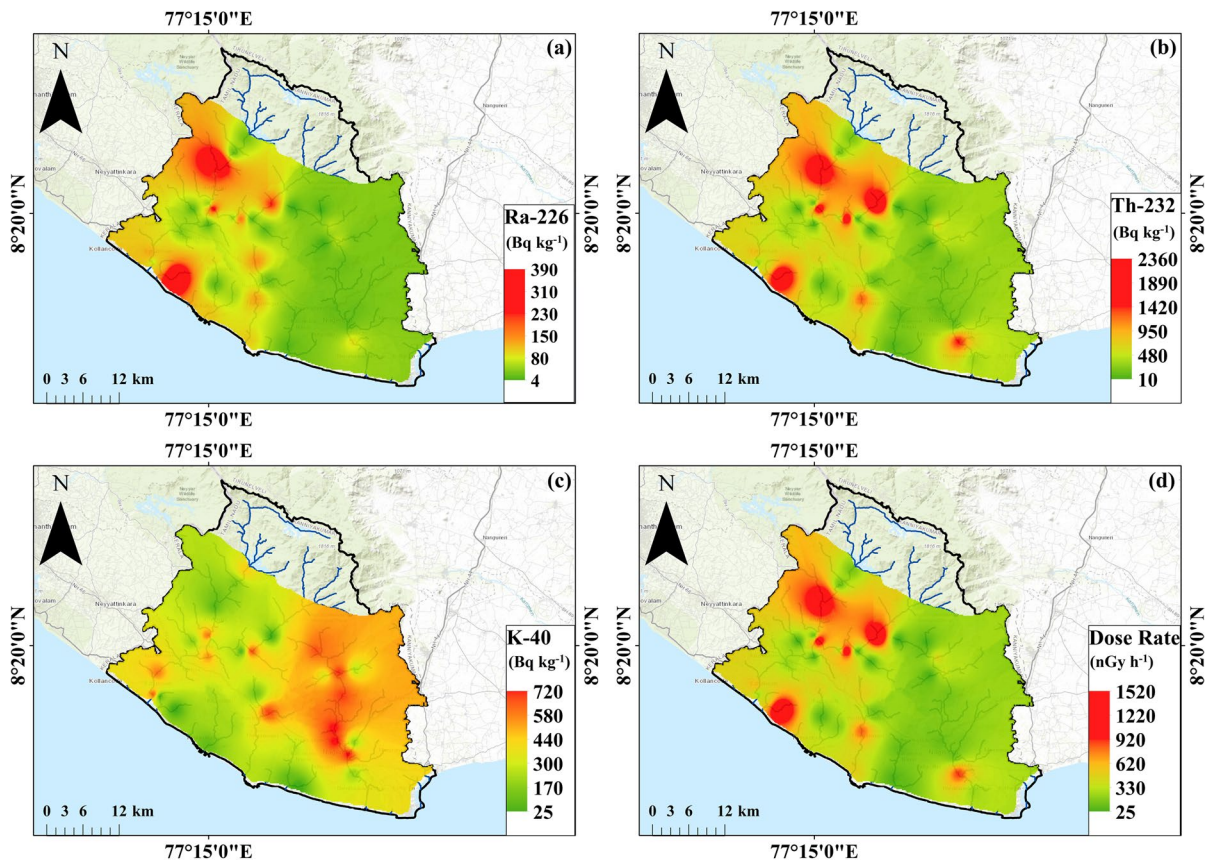


Fig. 4 Spatial distribution maps of activity concentrations of **a** ^{226}Ra , **b** ^{232}Th , and **c** ^{40}K . **d** Absorbed dose rate distribution map (Generated using ArcGIS v 10.6)

as well as a few other countries like Bangladesh, China, Egypt, Nigeria, Slovak Republic, Thailand, and United States are given in Table 2.

The radiological hazard parameters such as Ra_{eq} (Bq kg^{-1}), $AEDE_{out}$ (mSv y^{-1}), and $AEDE_{in}$ (mSv y^{-1}) were also estimated along with the absorbed dose rate using Eqs. 3, 4 and 5. The Ra_{eq} for the TR sediments ranged from 110 to 3574 Bq kg^{-1} with a mean of 1230 Bq kg^{-1} ; for the PR sediments, it ranged from 57 to 2070 Bq kg^{-1} with a mean of 520 Bq kg^{-1} ; and for the SS sediment samples, it ranged from 120 to 3465 Bq kg^{-1} with a mean of 910 Bq kg^{-1} . The mean Ra_{eq} of all the sediment samples was found to be 920 Bq kg^{-1} , which was relatively higher than the UNSCEAR world average value of 370 Bq kg^{-1} (Fig. 5). The annual effective dose equivalent outdoor ($AEDE_{out}$) and indoor ($AEDE_{in}$) values for the river and stream sediment samples from Kanyakumari were in the range of

0.03 to 1.9 mSv y^{-1} with a mean of 0.5 mSv y^{-1} and 0.1 to 7.4 mSv y^{-1} with a mean of 1.9 mSv y^{-1} , respectively. Both the $AEDE_{out}$ and $AEDE_{in}$ were higher than the world average values of 0.07 mSv y^{-1} and 0.45 mSv y^{-1} (UNSCEAR, 2008).

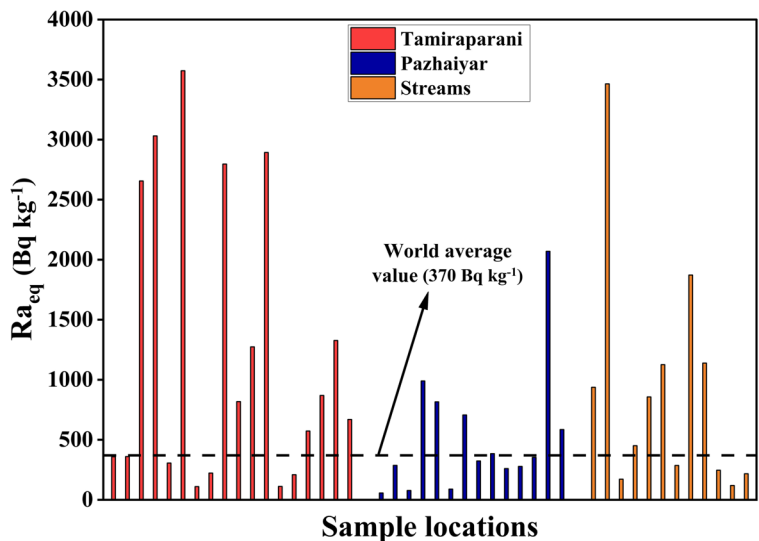
The absorbed dose rate as well as the activity concentration of radionuclides in the river and stream sediments of Kanyakumari were high relative to all the river sediments except for the ^{238}U and ^{232}Th activity concentrations of the Rushikulya and Mahanadi Rivers in Odisha (Table 2). The reported high concentrations of titanium (Ti) and cerium (Ce) in the Rushikulya and Mahanadi River sediments have been attributed to the presence of heavy minerals such as ilmenite (Ti dominant) and monazite (Ce dominant) (Mohanty et al., 2023). Our recent studies on the beach sands of Kanyakumari determined that the dose rate was mainly from ^{232}Th and the high concentrations of Ti and Ce in beach sands propounding

Table 2 Comparison of activity concentrations of ²²⁶Ra, ²³²Th, and ⁴⁰K and absorbed dose rate of the present study with sediments of other rivers of India and of other countries

River and country	Mean activity concentration (Bq kg ⁻¹)				Absorbed dose rate (nGy h ⁻¹)	Reference
	²³⁸ U	²²⁶ Ra	²³² Th	⁴⁰ K		
Brahmaputra River, Bangladesh		43	82	871	106	Khan et al. (2022)
Wei River, China	-	22	33	833	65	Lu et al. (2008)
Nile River, Egypt	16	-	13	200	24	El-Gamal et al. (2007)
Ogun River, Nigeria	-	13	12	500	64	Jibiri & Okeyode (2012)
Dudvah River, Slovak Republic		33	44	587	-	Frantisek et al. (2008)
Chao Phraya River, Thailand	60	-	65	432	85	Santawamaitre et al. (2011)
Reedy River (South Carolina), United States	38	21	45	609	63	Powell et al. (2007)
Rushikulya River (OD) ^a , India	100 ^b	-	540 ^b	-	-	Mohanty et al. (2023)
Mahanadi River (OD) ^a , India	330 ^b	-	2345 ^b	-	-	Mohanty et al. (2023)
Kallada River (KL) ^a , India	-	49	88	423	95	Venunathan et al. (2016)
Thamirabarani River (TN) ^a , India	-	41	52	838	85	Thangam et al. (2020)
Cauvery River (TN) ^a , India	-	32	61	144	58	Narayana et al. (2016)
Ponnaiyar River (TN) ^a , India	-	6	59	401	55	Ramasamy et al. (2011)
Beach sands, Kanyakumari, India	-	402	3970	160	2635	Natarajan et al. (2023a)
Tamiraparani River, Kanyakumari, India	-	100	773	339	527	Present study
Pazhaiyar River, Kanyakumari, India	-	33	313	512	226	Present study
Streams, Kanyakumari, India	-	95	557	211	289	Present study
World average	33	32	45	412	58	UNSCEAR (2008)

^aKL Kerala, OD Odisha, TN Tamil Nadu. ^bValues converted from µg g⁻¹ to Bq kg⁻¹ as per IAEA, 1990

Fig. 5 Radium equivalent activity for the sediment samples from Kanyakumari



the natural radiation were mainly due to ilmenite and monazite (Natarajan et al., 2023a, 2023b).

The respective absorbed dose rates for ²²⁶Ra and ²³²Th had a strong positive correlation ($R^2=0.78$

and 0.99) which may be due to the similar origins. The contribution of ²³²Th to the absorbed dose rate was 87%, which was similar to the contribution for the Kanyakumari beach sands (Natarajan et al.,

2023a). The highest ^{232}Th activity concentration was for sample TR-6 (Table 1), which was Paraliyar River bed sediment collected in close proximity to the Perunchanai Dam (Fig. 1b). The ^{226}Ra and ^{232}Th activity concentrations of samples TR-7 and TR-8 sharply decreased compared to TR-6 values whereas for TR-9 sample, the activity concentrations were somewhat lower compared to TR-6. There was no gradual increase or decrease in the activity concentration from the foothills of the catchment area reaching the mouth of the river rather; the ^{226}Ra and ^{232}Th activity concentrations fluctuated highly unlike the activity concentrations of ^{238}U , ^{232}Th , and ^{40}K in the sediments of the Ponnaiyar River (Ramasamy et al., 2011). Flow velocity of a river has a direct relationship to the sediment carrying capacity; when the flow velocity decreases, the river loses its ability to carry the heavy minerals first and a normal graded bedding depositional sequence is followed (sand at the bottom and mud at the top) (Earle, 2019). Bedrock exposure in the river channel may cause sediments to deposit in pockets and river erosional features like potholes were witnessed in upstream areas of rivers flowing in Kanyakumari. These are some of the factors that could control the uneven distribution of radionuclides along the river channels.

On the other hand, almost all the SS sediment samples from the small streams flowing adjacent to the agricultural lands showed an elevated activity concentration of ^{232}Th as well as the absorbed dose rate than UNSCEAR world average values (Table 1). Soil samples from other parts of Kanyakumari also showed a high-level activity concentration of ^{232}Th and an absorbed dose rate (Malathi et al., 2005). Similar observations paved a way to study the fate of radionuclides in food crops grown in the Kanyakumari region, since the radionuclides can transfer from soil to plant by root uptake. Major foods in the diet of Kanyakumari residents include rice and tapioca and the Th activity concentrations in both were reported to be higher than the activity concentrations of other radionuclides (Shanthi et al., 2009). For an adult in this region, the daily radionuclide intake and daily dose through ingestion of food crops were nearly 127.7 Bq day^{-1} and $2.3\text{ }\mu\text{Sv day}^{-1}$ which were relatively higher when compared to values for ingestion of food crops grown in areas where the background radiation is low (Shanthi et al., 2009).

Statistical approach

The standard deviation values were similar to or higher than the mean value for the activity concentration of the radionuclides as well as for the radiological hazard parameters, and this indicates a low degree of uniformity of the distribution of radionuclides. The overall kurtosis of ^{40}K was found to be platykurtic, suggesting a near uniform distribution, while the leptokurtic nature of the activity concentrations of ^{226}Ra and ^{232}Th and the absorbed dose rate shows more variance with infrequent extreme deviations (Fig. 6).

The skewness shows the asymmetry of the probability distribution. The ^{40}K activity concentration of the river and stream sediments showed a normal symmetrical distribution (Fig. 6c). However, the ^{226}Ra and ^{232}Th and absorbed dose rates were right-skewed with an asymmetric tail extending towards the values that were more positive. Based on the frequency distributions, about 75% of the activity concentration of ^{226}Ra , ^{232}Th , and ^{40}K for the collected samples were under 106 Bq kg^{-1} , 685 Bq kg^{-1} , and 586 Bq kg^{-1} (Fig. 6a, b, c), whereas 50% of the absorbed dose rates were in the range of 115 to 485 nGy h^{-1} (Fig. 6d).

The principal component analysis (PCA) is one of the most powerful mathematical tools to reduce the dimensionality of data sets and it helps in understanding the correlation of the different variables which could lead to source discrimination. To carry out the PCA and for an easy interpretation, varimax rotation using Kaiser normalization was applied which helps in maximizing the component loadings variance and eliminating invalid components (Dragović & Onjia, 2006). The factor analysis supports extracting the eigenvectors from the correlation matrix and the two significant components obtained are given in Table 3. The scree plot using eigenvalues for the sediment samples is shown in Fig. 7. The sharp falloff from the first to the second component (Fig. 7) indicated that the first component (PC 1) accounted for most of the data variability (Kumar et al., 2012). About 97.15% of the total variance was explained by these two components, PC 1 accounted for 86.80% and PC 2 accounted for 10.35%. The PC 1 was distinctive due to the positive loading of ^{226}Ra and ^{232}Th , whereas PC 2 was controlled by the positive loading of ^{40}K (Table 3).

Figure 8 shows the effect of components PC 1 and PC 2 on the radionuclides ^{226}Ra , ^{232}Th , and

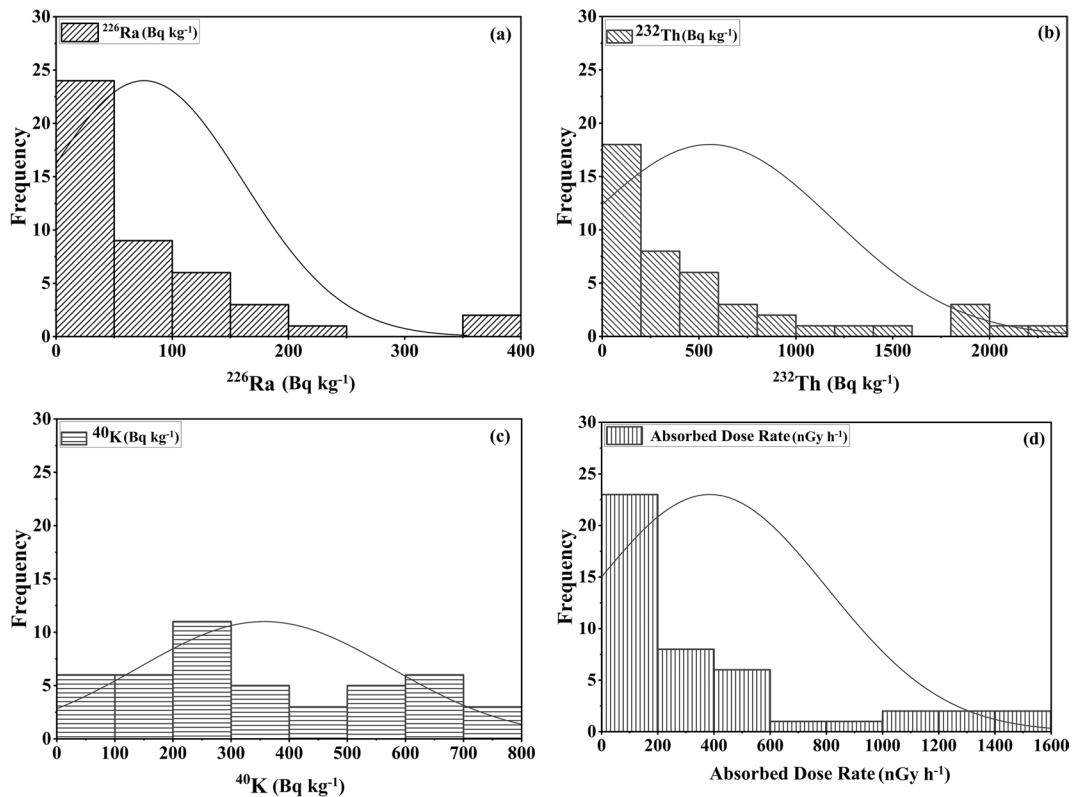


Fig. 6 Frequency distributions of activity concentrations of a ^{226}Ra , b ^{232}Th , and c. ^{40}K . d Absorbed dose rate frequency distribution ($n=44$)

Table 3 Varimax rotated components of the variable

Variable	Component 1	Component 2
^{226}Ra	0.37	0.05
^{232}Th	0.40	0.08
^{40}K	-0.23	0.97

^{40}K of sediments from selected sampling locations as the factor score. The factor score can distinguish the influence of each radionuclide; here, PC 1 was the loading of ^{226}Ra and ^{232}Th and PC 2 was influenced by ^{40}K . The highest PC 1 scores can be seen in the sediment samples collected upstream for the TR (TR-3, -4, and -6) (Fig. 8a), and that shows these sediment samples were enriched with ^{226}Ra and ^{232}Th . Most of the sediment samples from the PR had high PC 2 scores (Fig. 8b) due to the direct influence of the low activity concentration of ^{226}Ra and the high activity concentration of ^{40}K . Nearly all SS sediment samples showed similar factor scores for both PC 1

and PC 2 except SS-2 (Fig. 8c), which was controlled by the high ^{232}Th activity concentration (Table 1). Figure 9 shows the cluster plot generated for the sediment samples using the PCA results. The sediment samples from the rivers and seasonal streams are grouped separately and the ellipses represent the 95% confidence level. The overlapping of all three groups might indicate a similar origin for the sediments.

Conclusion

The activity concentrations of the natural radionuclides ^{226}Ra , ^{232}Th , and ^{40}K and their associated risk parameters were evaluated for river and stream sediment samples collected in the Kanyakumari HBNRA. The present investigation, the first of its kind for the Kanyakumari area, revealed that the mean activity concentrations of ^{226}Ra and ^{232}Th for the sediments were relatively higher than the UNSCEAR world average values. The radiological hazard indices

Fig. 7 Scree plot of eigenvalues for Kanyakumari River and stream sediments

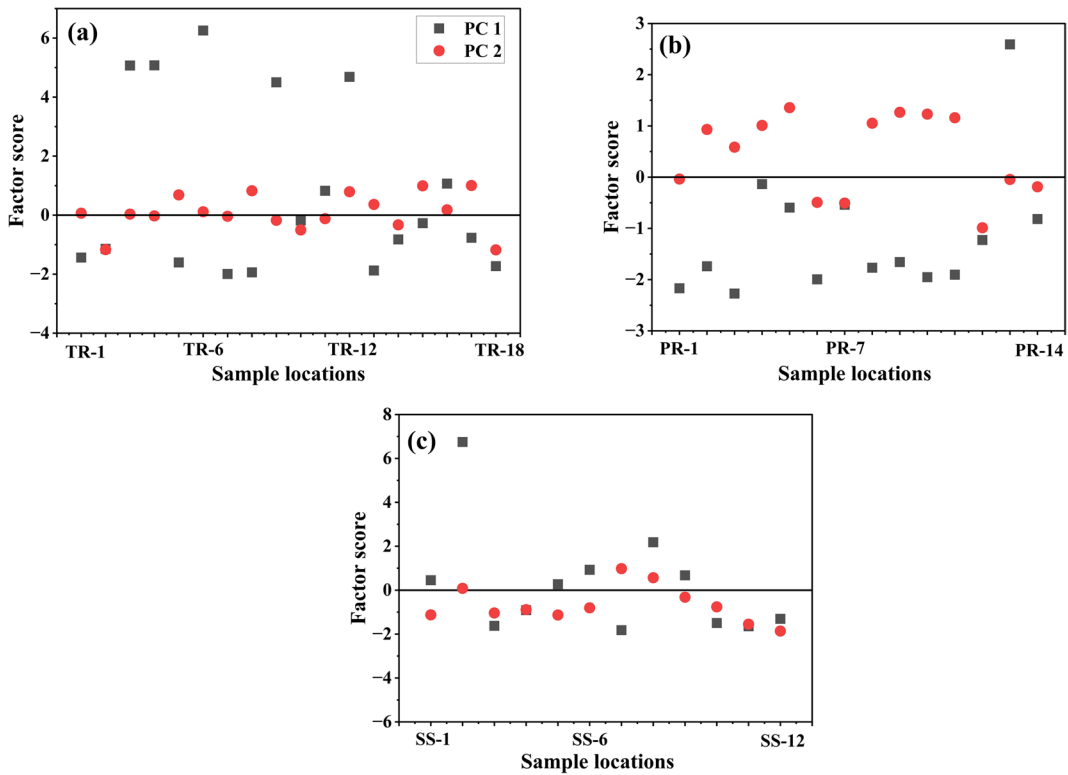
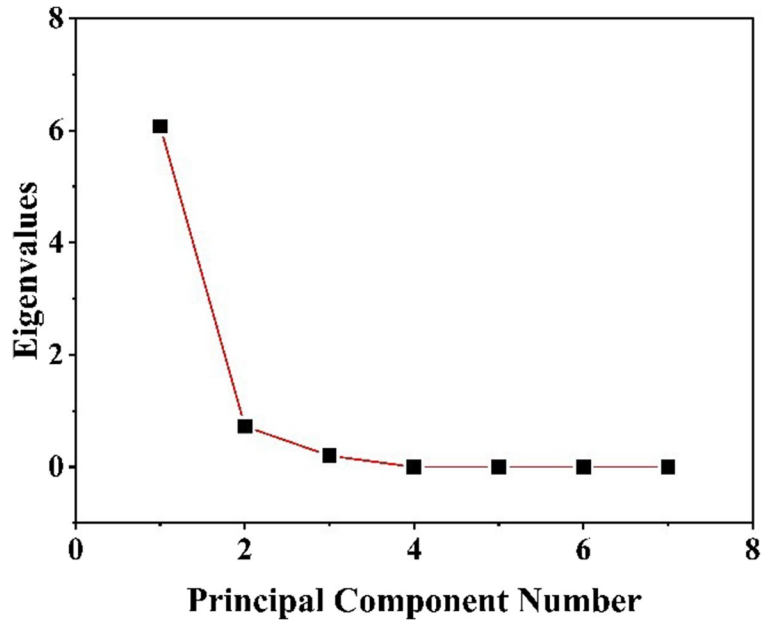
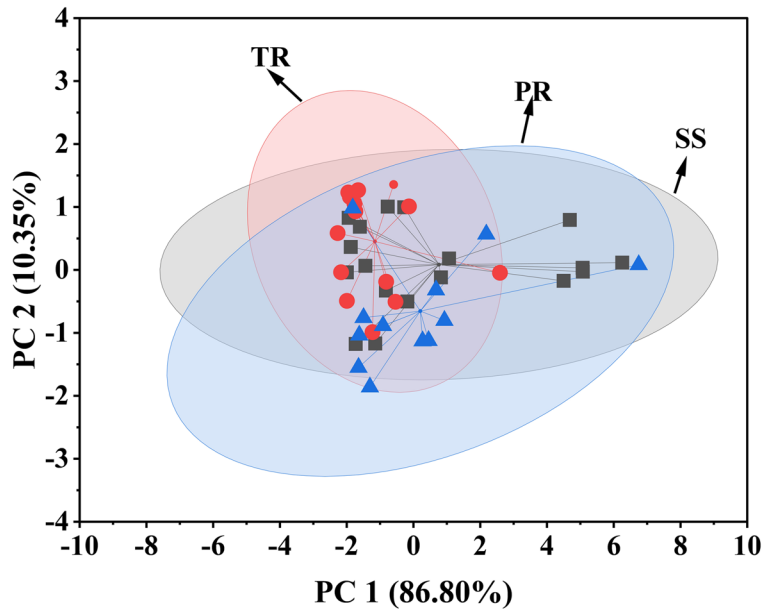


Fig. 8 Factor score of sediments from **a** TR, **b** PR, and **c** SS (TR, Tamiraparani River; PR, Pazhaiyar River; SS, seasonal stream)

Fig. 9 Principal component analysis (PCA) with the cluster of radionuclides (TR, Tamiraparani River; PR, Pazhaiyar River; SS, seasonal stream)



such as absorbed dose rate (D), Ra_{eq} , $AEDE_{out}$, and $AEDE_{in}$ were estimated and the means of all these indices were found to be higher than the UNSCEAR world average values. The high $^{232}\text{Th}/^{226}\text{Ra}$ ratio in the sediments could explain the removal of ^{226}Ra in the particulate phase due to the terrestrial oxidizing environment and the high ratios supported the presence of Th-bearing minerals. Due to the presence of clay minerals, the $^{232}\text{Th}/^{40}\text{K}$ ratio of PR sediments was relatively lower than the TR and SS sediments; however, the $^{232}\text{Th}/^{40}\text{K}$ ratio was higher than the world average. The results of the multivariate statistical analysis of the sediments were able to explain the uneven distribution of the radionuclides, even though the sources of the sediments were similar. Based on these findings, the Kanyakumari sediments were concluded to be enriched with ^{232}Th and that had a significant influence on the natural radioactivity of the area. This study is expected to be useful in understanding whether these river sediments pose any radiological risk when they are used for construction purposes. The results can help in understanding the source of natural radionuclides deposited along the Kanyakumari coast, and a geochemical and mineralogical study would provide further details.

Acknowledgements Thennaarassan Natarajan is thankful to the Tokyo Metropolitan Government, Tokyo, Japan, for the award of the doctoral fellowship “Tokyo Human

Resources Fund for City Diplomacy” for study at Tokyo Metropolitan University. Thennaarassan Natarajan also thanks the Institute for Radiological Sciences, National Institutes for Quantum Science and Technology (QST) Chiba, Japan, for the award of QST Research Assistant. All authors thank Dr. R. Kalaivanan, Dr. M. Sridharan, and Mr. S. Harikrishnan, Pondicherry University, for their help during field work and sample collection.

Author contribution Thennaarassan Natarajan: methodology, software, investigation, data curation, formal analysis, writing—original draft preparation, writing—reviewing and editing. Sarata Kumar Sahoo: methodology, investigation, supervision, formal analysis, validation, resources, funding acquisition, writing—reviewing and editing. Kazumasa Inoue: supervision, resources, funding acquisition, writing—reviewing and editing. Hideki Arae: formal analysis, validation. Tatsuo Aono: writing—reviewing and editing. Masahiro Fukushi: writing—reviewing and editing.

Funding This research was partially supported by the Japan Society for Promotion of Science (JSPS) core-to-core program (Grant Number: JPJSCCB20210008).

Data availability The data underlying this article will be shared on reasonable request to the corresponding author.

Declarations

Ethical approval Not applicable.

Competing interests The authors declare no competing interests.

References

- CGWB (Central Groundwater Board of India) (2008). District groundwater brochure Kanyakumari district, Tamil Nadu. Accessed 8 July 2023. <http://cgwb.gov.in/node/1446>.
- Dragović, S., & Onjia, A. (2006). Classification of soil samples according to their geographic origin using gamma-ray spectrometry and principal component analysis. *Journal of Environmental Radioactivity*, 89(2), 150–158. <https://doi.org/10.1016/j.jenvrad.2006.05.002>
- Earle, S. (2019). *Physical geology*, 2nd edn. BC campus, British Columbia. Retrieved from <https://opentextbc.ca/physicalgeology2ed/>
- El-Gamal, A., Nasr, S., & El-Taher, A. (2007). Study of the spatial distribution of natural radioactivity in the upper Egypt Nile River sediments. *Radiation Measurements*, 42(3), 457–465. <https://doi.org/10.1016/j.radmeas.2007.02.054>
- Forster, L., Forster, P., Lutz-Bonengel, S., Willkomm, H., & Brinkmann, B. (2002). Natural radioactivity and human mitochondrial DNA mutations. *Proceedings of the National Academy of Sciences*, 99(21), 13950–13954. <https://doi.org/10.1073/pnas.202400499>
- Frantisek, D., Maria, B., & Durecova, A. (2008). Intercomparison exercise on the determination of radionuclides in sediment from the Dudvah river. *Applied Radiation and Isotopes*, 66(11), 1706–1710. <https://doi.org/10.1016/j.apradiso.2007.11.021>
- Ghiassi-nejad, M., Mortazavi, S. M., Cameron, J. R., Niroomand-rad, A., & Karam, P. A. (2002). Very high background radiation areas of Ramsar, Iran: Preliminary biological studies. *Health Physics*, 82(1), 87–93. <https://doi.org/10.1097/00004032-200201000-00011>
- Van Gosen, B.S., Fey, D.L., Shah, A.K., Verplanck, P.L., & Hoefen, T.M. (2014). Deposit model for heavy-mineral sands in coastal environments. In *Mineral deposit models for resource assessment; U.S. Geological Survey Scientific Investigations Report*; U.S. Geological Survey: Reston, VA, USA. <https://doi.org/10.3133/sir20105070L>
- Hassan, N. M., Ishikawa, T., Hosoda, M., Sorimachi, A., Tokonami, S., Fukushi, M., & Sahoo, S. K. (2010). Assessment of the natural radioactivity using two techniques for the measurement of radionuclide concentration in building materials used in Japan. *Journal of Radioanalytical and Nuclear Chemistry*, 283, 15–21. <https://doi.org/10.1007/s10967-009-0050-6>
- IAEA (International Atomic Energy Agency), (1990). Construction and use of calibration facilities for radiometric field equipment. IAEA 1990 *Technical Reports Series No. 309*, Vienna, Austria.
- Jibiri, N. N., & Okeyode, I. C. (2012). Evaluation of radiological hazards in the sediments of Ogun river. *South-Western Nigeria. Radiation Physics and Chemistry*, 81(2), 103–112. <https://doi.org/10.1016/j.radphyschem.2011.10.002>
- Khan, R., Islam, H. M. T., Apon, M. A. S., Islam, A. R. M. T., Habib, M. A., Phoungthong, K., Idris, A. M., & Techato, K. (2022). Environmental geochemistry of higher radioactivity in a transboundary Himalayan river sediment (Brahmaputra, Bangladesh): Potential radiation exposure and health risks. *Environmental Science and Pollution Research*, 29, 57357–57375. <https://doi.org/10.1007/s11356-022-19735-5>
- Kumar, A., Joshi, V. M., Mishra, M. K., Karpe, R., Rout, S., Narayanan, U., Tripathi, R. M., Singh, J., Kumar, S., Hegde, A. G., & Kushwaha, H. S. (2012). Distribution, enrichment and principal component analysis for possible sources of naturally occurring and anthropogenic radionuclides in the agricultural soil of Punjab state. *India. Radiation Protection Dosimetry*, 150(1), 71–81. <https://doi.org/10.1093/rpd/ncr366>
- Li, J., & Heap, A. D. (2011). A review of comparative studies of spatial interpolation methods in environmental sciences: Performance and impact factors. *Ecological Informatics*, 6(3–4), 228–241. <https://doi.org/10.1016/j.ecoinf.2010.12.003>
- Lu, X., Zhang, X., & Wang, F. (2008). Natural radioactivity in sediment of Wei River, China. *Environmental Geology*, 53, 1475–1481. <https://doi.org/10.1007/s00254-007-0756-0>
- Malathi, J., Selvasekarapandian, S., Brahmanandhan, G. M., Khanna, D., Meenakshisundaram, V., & Mathiyarsu, R. (2005). Study of radionuclide distribution around Kudankulam nuclear power plant site (Agastheeswaram taluk of Kanyakumari district, India). *Radiation Protection Dosimetry*, 113(4), 415–420. <https://doi.org/10.1093/rpd/nch472>
- Mohanty, A. K., Das, S. K., Van, K. V., Sengupta, D., & Saha, S. K. (2003). Radiogenic heavy minerals in Chhatrapur beach placer deposit of Orissa, southeastern coast of India. *Journal of Radioanalytical and Nuclear Chemistry*, 258, 383–389. <https://doi.org/10.1023/A:1026202224700>
- Mohanty, S., Khan, R., Tamim, U., Adak, S., Bhunia, G. S., & Sengupta, D. (2023). Geochemical and Radionuclide studies of sediments as tracers for enrichment of beach and alluvial placers along the eastern coast of India. *Regional Studies in Marine Science*, 63, 103003. <https://doi.org/10.1016/j.rsma.2023.103003>
- Narayana, Y., Kaliprasad, C. S., & Sanjeev, G. (2016). Natural radionuclide levels in sediments of cauvery riverine environment. *Radiation Protection Dosimetry*, 171(2), 229–233. <https://doi.org/10.1093/rpd/ncw064>
- Natarajan, T., Inoue, K., & Sahoo, S. K. (2023b). Rare earth elements geochemistry and ²³⁴U/²³⁸U, ²³⁵U/²³⁸U isotope ratios of the Kanyakumari beach placer deposits: Occurrence and provenance. *Minerals*, 13(7), 886. <https://doi.org/10.3390/min13070886>
- Natarajan, T., Sahoo, S.K., Nakajima, T., Veerasamy, N., Yamazaki, S., Inoue, K., & Ramola, R.C. (2023). Distribution of ²²⁶Ra, ²³²Th and ⁴⁰K in Kanyakumari beach placer deposits along Tamil Nadu coast, India. *Journal of Radioanalytical and Nuclear Chemistry*. <https://doi.org/10.1007/s10967-023-08940-2>
- Omori, Y., Sorimachi, A., Gun-Aajav, M., Enkhgerel, N., Munkherdene, G., Oyunbolor, G., Shajbalidir, A., Palam, E., & Yamada, C. (2019). Gamma dose rate distribution in the Unegt subbasin, a uranium deposit area in Dornogobi Province, southeastern Mongolia. *Environmental Science and Pollution Research*, 26, 33494–33506. <https://doi.org/10.1007/s11356-019-06420-3>
- Powell, B. A., Hughes, L. D., Soreefan, A. M., Falta, D., Wall, M., & DeVol, T. A. (2007). Elevated concentrations of

- primordial radionuclides in sediments from the Reedy River and surrounding creeks in Simpsonville, South Carolina. *Journal of Environmental Radioactivity*, 94(3), 121–128. <https://doi.org/10.1016/j.jenvrad.2006.12.013>
- Punniyakotti, J., & Ponnusamy, V. (2018). Environmental radiation and potential ecological risk levels in the intertidal zone of southern region of Tamil Nadu coast (HBRAs) India. *Marine Pollution Bulletin*, 127, 377–386. <https://doi.org/10.1016/j.marpolbul.2017.11.026>
- Raja, V., Sahoo, S. K., Sreekumar, K., & Neelakanta, M. A. (2021). High background radiation places and spatial distribution of uranium in groundwater of monazite placer deposit in Kanniyakumari district, Tamil Nadu, India. *Journal of Radioanalytical and Nuclear Chemistry*, 328, 925–939. <https://doi.org/10.1007/s10967-021-07727-7>
- Rajesh, H. M., Santosh, M., & Yoshikura, S. (2011). The Nagercoil charnockite: A magnesian, calcic to calc-alkalic granitoid dehydrated during a granulite-facies metamorphic event. *Journal of Petrology*, 52(2), 375–400. <https://doi.org/10.1093/petrology/egq084>
- Ramasamy, V., Suresh, G., Meenakshisundaram, V., & Ponnusamy, V. (2011). Horizontal and vertical characterization of radionuclides and minerals in river sediments. *Applied Radiation and Isotopes*, 69(1), 184–195. <https://doi.org/10.1016/j.apradiso.2010.07.020>
- Rupasinghe, M. S., Gocht, W., & Dissanayake, C. B. (1983). The genesis of thorium-rich monazite placer deposits in Sri Lanka. *Journal of the National Science Foundation of Sri Lanka*, 11(1), 99–110. <https://doi.org/10.4038/jnsfr.v11i1.8405>
- Sahoo, S. K., Zunic, Z. S., Veerasamy, N., Natarajan, T., Zhukovsky, M., Jovanovic, P., Veslinovic, N., Janicijevic, A., Onischenko, A., Yarmoshenko, I., & Ramola, R. C. (2023). Distribution of radionuclides and associated radiological risk assessment of soils from Niška Banja, Serbia. *Journal of Radioanalytical and Nuclear Chemistry*. <https://doi.org/10.1007/s10967-023-09017-w>
- Sakr, S., Inoue, K., Mohamed, A., Ahmed, A. A., ElFeky, M. G., Saleh, G. M., Kamar, M. S., Arae, H., Aono, T., & Sahoo, S. K. (2023). Distribution of natural radionuclides in NORM samples from North Abu Rusheid area. *Egypt. Journal of Environmental Radioactivity*, 266, 107240. <https://doi.org/10.1016/j.jenvrad.2023.107240>
- Santawamaitre, T., Malain, D., Al-Sulaiti, H. A., Mathews, M., Bradley, D. A., & Regan, P. H. (2011). Study of natural radioactivity in riverbank soils along the Chao Phraya river basin in Thailand. *Nuclear Instruments and Methods in Physics Research - Section A*, 652(1), 920–924. <https://doi.org/10.1016/j.nima.2010.10.057>
- Santosh, M., Yokoyama, K., Biju-Sekhar, S., & Rogers, J. J. W. (2003). Multiple tectonothermal events in the granulite blocks of Southern India revealed from EPMA dating: Implications on the history of Supercontinents. *Gondwana Research*, 6(1), 29–63. [https://doi.org/10.1016/S1342-937X\(05\)70643-2](https://doi.org/10.1016/S1342-937X(05)70643-2)
- Shanthi, G., Maniyan, C. G., Raj, G. A. G., & Kumaran, J. T. T. (2009). Radioactivity in food crops from high background radiation area in southwest area. *Current Science*, 97(9), 1331–1335.
- Singh, H. N., Shanker, D., Neelakandan, V. N., & Singh, V. P. (2007). Distribution patterns of natural radioactivity and delineation of anomalous radioactive zones using in situ radiation observations in Southern Tamil Nadu. *India. Journal of Hazardous Material*, 141(1), 264–272. <https://doi.org/10.1016/j.jhazmat.2006.06.118>
- Sulekha Rao, N., & Misra, S. (2009). Sources of monazite sand in southern Orissa beach placer, eastern India. *Journal of the Geological Society of India*, 74, 357–362. <https://doi.org/10.1007/s12594-009-0140-7>
- Thangam, V., Rajalakshmi, A., Chandrasekaran, A., & Jananee, B. (2020). Measurement of natural radioactivity in river sediments of Thamirabarani, Tamil Nadu, India using gamma ray spectroscopic technique. *International Journal of Environmental Analytical Chemistry*, 102(2), 422–433. <https://doi.org/10.1080/03067319.2020.1722815>
- UNSCEAR (United Nations Scientific Committee on the Effects of Atomic Radiation) (2008) Sources and effects of ionizing radiation. Annex B - Exposures of the public and workers from various sources of radiation, Vol. 1, UNSCEAR. (2008). Report. United Nations, New York
- UNSCEAR (United Nations Scientific Committee on the Effects of Atomic Radiation) (2000) Sources and effects of ionizing radiation. Annex B - Exposures from the Natural Radiation Sources Vol. 1, 84 – 141, UNSCEAR 2000 Report, United Nations, New York
- Veerasamy, N., Sahoo, S. K., Inoue, K., Arae, H., & Fukushima, M. (2020). Geochemical behavior of uranium and thorium in sand and sandy soil samples from a natural high background radiation area of the Odisha coast, India. *Environmental Science and Pollution Research*, 27, 31339–31349. <https://doi.org/10.1007/s11356-020-09370-3>
- Veerasamy, N., Kasar, S., Murugan, R., Inoue, K., Natarajan, T., Ramola, R. C., Fukushima, M., & Sahoo, S. K. (2023). $^{234}\text{U}/^{238}\text{U}$ disequilibrium and $^{235}\text{U}/^{238}\text{U}$ ratios measured using MC-ICP-MS in natural high background radiation area soils to understand the fate of uranium. *Chemosphere*, 323, 138217. <https://doi.org/10.1016/j.chemosphere.2023.138217>
- Venunathan, N., Kaliprasad, C. S., & Narayana, Y. (2016). Natural radioactivity in sediments and river bank soil of Kallada river of Kerala, South India and associated radiological risk. *Radiation Protection Dosimetry*, 171(2), 271–276. <https://doi.org/10.1093/rpd/ncw073>

Publisher's Note Springer Nature remains neutral with regard to jurisdictional claims in published maps and institutional affiliations.

Springer Nature or its licensor (e.g. a society or other partner) holds exclusive rights to this article under a publishing agreement with the author(s) or other rightsholder(s); author self-archiving of the accepted manuscript version of this article is solely governed by the terms of such publishing agreement and applicable law.